biosensors

MDPI

Article

An Innovative Polymer-Based Electrochemical Sensor Encrusted with Tb Nanoparticles for the Detection of Favipiravir: A Potential Antiviral Drug for the Treatment of COVID-19

Marwa F. B. Ali [1], Roshdy E. Saraya [2], Sami El Deeb [3,4,*], Adel Ehab Ibrahim [2,4] and Baher I. Salman [5]

[1] Department of Pharmaceutical Analytical Chemistry, Faculty of Pharmacy, Assiut University, Assiut 71526, Egypt
[2] Pharmaceutical Analytical Chemistry Department, Faculty of Pharmacy, Port-Said University, Port Said 42526, Egypt
[3] Institute of Medicinal and Pharmaceutical Chemistry, Teschnische Universität Braunschweig, 38106 Braunschweig, Germany
[4] Natural and Medical Sciences Research Center, University of Nizwa, Birkat Al Mauz, P.O. Box 33, Nizwa 616, Oman
[5] Pharmaceutical Analytical Chemistry Department, Faculty of Pharmacy, Al-Azhar University, Assiut Branch, Assiut 71524, Egypt
* Correspondence: s.eldeeb@tu-bs.de; Tel.: +49-531-391-7301

Abstract: An innovative polymer-based electro-sensor decorated with Tb nanoparticles has been developed for the first time. The fabricated sensor was utilized for trace determination of Favipiravir (FAV), a recently US FDA-approved antiviral drug for the treatment of COVID-19. Different techniques, including ultraviolet-visible spectrophotometry (UV-VIS), cyclic voltammetry (CV), scanning electron microscope (SEM), X-ray Diffraction (XRD) and electrochemical impedance spectroscopy (EIS), were applied for the characterization of the developed electrode Tb_{NPs}@ poly m-THB/PGE. Various experimental variables, including pH, potential range, polymer concentration, number of cycles, scan rate and deposition time, were optimized. Moreover, different voltammetric parameters were examined and optimized. The presented SWV method showed linearity over the range of 10–150 × 10^{-9} M with a good correlation coefficient (R = 0.9994), and the detection limit (LOD) reached 3.1 × 10^{-9} M. The proposed method was applied for the quantification of FAV in tablet dosage forms and in human plasma without any interference from complex matrices, obtaining good % recovery results (98.58–101.93%).

Keywords: Favipiravir; m-THB polymer; Tb nanoparticles; COVID-19; human plasma analysis

check for updates

Citation: Ali, M.F.B.; Saraya, R.E.; El Deeb, S.; Ibrahim, A.E.; Salman, B.I. An Innovative Polymer-Based Electrochemical Sensor Encrusted with Tb Nanoparticles for the Detection of Favipiravir: A Potential Antiviral Drug for the Treatment of COVID-19. *Biosensors* **2023**, *13*, 243. https://doi.org/10.3390/bios13020243

Received: 27 December 2022
Revised: 26 January 2023
Accepted: 7 February 2023
Published: 8 February 2023

Copyright: © 2023 by the authors. Licensee MDPI, Basel, Switzerland. This article is an open access article distributed under the terms and conditions of the Creative Commons Attribution (CC BY) license (https://creativecommons.org/licenses/by/4.0/).

1. Introduction

Favipiravir (FAV), 6-fluoro-3-hydroxy-2-pyrazinecarboxamide, is a promising antiviral pro-drug belonging to the RNA polymerase inhibitors. It was first introduced in Japan in 2014 as an anti-influenza agent, and it was also applied to treat other viruses [1]. In 2019, it was proven to be safe and effective against COVID-19, a global pandemic with outbreaks all over the world, as the World Health Organization (WHO) officially declared in March 2020. COVID-19 causes severe respiratory syndrome leading to a serious disease that affects different organs, including the kidneys, liver and central nervous system [2].

Although the pandemic crest has diminished lately due to several considerations, such as global vaccination and enhanced health awareness, however, its endemicity is said to be meaningless or at least only transitional. Expectations for infection spikes are high, which may be owed to the removal of restrictive measures as well as viral mutations [3,4]. Therefore, it was recommended to establish a sensitive, cost-effective and selective analytical method for the estimation of COVID-19 defense drugs such as FAV in biological fluids for routine drug quality control and further clinical studies' monitoring.

Although different analytical methods were published for the estimation of FAV, including spectrophotometric and spectrofluorimetric [5–9], thin layer chromatography [10,11], and liquid chromatography methods [5,7,12–17]. However, only a few voltammetric and electrochemical methods have been reported for the estimation of FAV till now [18–23]. Electrochemical techniques are currently more frequently used due to their simplicity, sensitivity, environment-friendly and ready availability. Besides, varying modifications of carbon-based electrodes have currently attracted considerable attention, where different nanomaterials [24,25] could be utilized for the detection of several analytes in complex matrices, such as pharmaceutical formulations and biological fluids. A pencil graphite electrode (PGE) is a working electrode that is commonly used currently. This can be attributed to its superb electrochemical properties like high conductivity, low cost, simplicity in modification and wide commercial availability [26–28]. Henceforth, it was recommended to establish a sensitive, selective and cost-effective electrochemical analytical approach for the estimation of FAV in human plasma for drug monitoring and further clinical studies.

Moreover, electro-polymerization has drawn great attention recently as one promising approach in electrochemistry [29]. Polymer-modified electrodes are used in the manufacturing of batteries or supercapacitors, organic light-emitting diodes and biosensors. The deposited polymers on the substrate surface own many properties like advanced electrical conductivity, redox mediating capabilities and specific adhesive and/or binding properties. These polymers are promising in electrode modification because it generally results in creating polymer film which is uniform and strongly adherent to the electrode surface [30]. Conducting polymers with extended π-π conjugated systems have been used in the synthesis and preparation of various electrochemical sensors [31–33] owing to their high conductivity and their redox properties. In addition, polymerization using polyhydroxy aromatic compounds has shown good stability, reproducibility, more active surface area and homogeneity in electrochemical deposition [34]. In the represented research, innovative polymer layers were created for the first time via utilizing phloroglucinol, a trihydroxy benzene compound (m-THB), which was electropolymerized in order to form electro-active layers on the surface of a solid surface of PGE.

Additional enhancement of the electrode activity and sensitivity was accomplished by the integration of metal nanostructures. In this article, we investigate the behavior of terbium nanocomposites. Terbium (Tb) is one of the lanthanide metals that has the ability to create more electronic charges or holes, efficiently generating an electron transfer pathway due to possessing two states of valence (Tb^{3+} and Tb^{4+}). Hence, the incorporation of Tb^{3+} nanoparticles (Tb_{NPS}) into any electrode modification is successfully enhancing the electronic conductivity, electrocatalytic activity, general electrochemical behavior, overall electrochemical performance and hence method sensitivity [35–37]. The incorporation of m-THB polymerized layers and Tb_{NPS} not only improves polymer characteristics but also provides excellent performance by increasing the active sites of the electrode surface utilizing these hybrid components.

Herein, a new strategy was introduced involving the design of the hybrid nanostructure composed of m-THB polymer layers over the PGE surface. Further, the incorporation of Tb_{NPS} overlaying the electro-active polymer layers was performed. The prepared electrode was characterized by UV-VIS spectrophotometry, scanning electron microscope (SEM), CV, SWV, and EIS methods. Besides, the modified sensor's electrochemical performance was considered in monitoring the electro-oxidation of FAV in human plasma and tablets. The proposed SWV method is simple, highly sensitive and can be recommended for therapeutic drug monitoring (TDM) and various clinical laboratories for further pharmacokinetic studies.

2. Materials and Methods

2.1. Materials

FAV (purity = 99.0%) authentic standard was obtained from EIPICo. (Tenth of Ramadan City, Egypt). Avipiravir® tablets (200 mg of FAV per tablet) were supplied from EVA Pharm (Giza, Egypt).

All chemicals and solvents were of analytical grades. Terbium chloride (III) hexahydrate ($TbCl_3 \cdot 6H_2O$), phloroglucinol (m-trihydroxy benzene, m-THB), potassium chloride, potassium ferrocyanide were obtained from Sigma–Aldrich. HPLC grade methanol was obtained from Sigma–Aldrich Co. (St. Louis, MO, USA). Phosphate buffer (0.1 M, pH 4.0–9.0) was prepared using sodium dihydrogen phosphate and di sodium hydrogen phosphate (El-Nasr Pharmaceutical Chemicals Co., Cairo, Egypt); pH was adjusted by 0.2 M NaOH. Rotring (HB) pencil leads (0.5 mm × 60 mm) were purchased from a local market.

Blank human plasma samples (fresh frozen plasma, B-Rh+) were supplied from Assiut University Hospitals Blood Bank (Assiut, Egypt).

2.2. Instruments

Voltammetric measurements were done using a Princeton VersaSTAT MC (VersaSTAT 3, model RE-1, Princeton Applied Research, AMETEK, Easttown Township, PA, USA), which consists of a 3-electrode electroanalytical cell (Ag/AgCl, 3 M KCl reference electrode, a platinum wire auxiliary electrode and PGE either bare or modified was a working electrode). Ultrasonic cleaner (Cole-Parmer, Chicago, IL, USA), Sartorious handy balance-H51 (Hannover, Germany), Hanna pH meter HI 4222 (Hanna Instruments Brazil, Sao Paulo, Brazil), Boeco laboratory centrifuge U-320®(, Hamburg, Germany), FALC vortex-MIX (FALC Instruments, Treviglio, Italy), and Scanning electron microscope; SEM (JEOL JSM-5400 LV instrument, Oxford, MO, USA) were used. UV–VIS spectra of the modified layers were recorded using a UV-visible spectrophotometer (UV-1601PC, Shimadzu, Kyoto, Japan) with 1.0 cm quartz cells. The X-ray powder diffraction was measured using a Philips X-ray PW 1710 with Cu Ka radiation (l 1/4 1.5405 °A) with 40 kV and 30 mA. The scanning rate was maintained at 0.06 scans per minute, in the 2q range of 4–80.

2.3. Standard and Reagent Solutions

A standard solution of FAV (5×10^{-6} M) was prepared in double distilled water. Phloroglucinol (m-trihydroxy benzene; m-THB) solution (32×10^{-3} M) and Tb (III) solution (500×10^{-3} M) were formed in double distilled water. Further dilutions were done using the same solvent to investigate the optimum concentration for the polymerization of m-THB and the optimum concentration for the electro-deposition of Tb.

2.4. Fabrication of Tb_{NPS}@ Poly m-THB/PGE

To fabricate the presented electrode, the PGE surface was first washed with double distilled water before use. Further, an electro-polymerization of m-THB was established using 8×10^{-3} M of m-THB solution in phosphate buffer (0.1 M, pH 7) through multiple cyclic voltammetry for 10 cycles using a potential range of −0.9–+1.75 V and scanning rate of 0.1 Vs^{-1}. The electrode was denoted as poly m-THB/PGE. Furthermore, the electrode was submerged in an electrochemical cell having Tb (III) chloride solution (125×10^{-3} M), which was electro-deposited using a potential at −1.2 V for 80 s. The fabricated Tb_{NPs}@ poly m-THB/PGE electrode was further characterized and checked by UV-Visible spectrophotometry, CV, SEM and EIS.

2.5. Analytical Procedures for Estimation of FAV

2.5.1. General Analytical Procedure

An appropriate volume of FAV (5×10^{-6} M) standard or sample solution was added into an electrochemical cell filled with 0.1 M phosphate buffer (pH 7) as a supporting electrolyte. The electrochemical performance of FAV using bare and modified PGE was studied using CV and SWV techniques. The experimental variables of the developed method in terms of m-THB polymerization, Tb_{NPs} electro-deposition and the optimum electrolyte pH were studied. Moreover, various SWV parameters were studied, including deposition time, frequency, initial potential and step and pulse height.

2.5.2. Procedure for Estimation of FAV in Tablets

Ten Avipiravir® tablets (200 mg per tablet) were weighed, crushed finally and thoroughly mixed. Then, an adequate weight equivalent to 10.0 mg FAV was transferred into a volumetric flask and dissolved into 50 mL of double distilled water. The solution was sonicated for about 20 min, followed by filtration, then the volume was made up to 100 mL with double distilled water to get a concentration of 100 μg mL^{-1}. The developed SWV method was then carried out as mentioned above.

2.5.3. Estimation of FAV in Human Plasma

In a centrifuge tube, 1.0 mL of human plasma was spiked with an adequate amount of FAV solution, and the volume was then furtherly made up to 10 mL using methanol. The mixture was vortexed for 30 s and then centrifuged for 35 min (3500 rpm). The resultant supernatant was collected, and appropriate volumes were added to the electrochemical cell. The voltammograms of SWV were recorded for FAV using the modified Tb_{NPs}@ poly m-THB/PGE electrode under the optimum experimental conditions. A blank measurement was established in the same way but without the drug. In addition, required dilutions from this supernatant were made using the selected supporting electrolyte. The study was performed following the relevant faculty laws and guidelines, as well as the research ethics committee.

2.6. Characterization of Tb_{NPs}@ Poly m-THB/PGE

The developed electrode was morphologically characterized using SEM and the modified polymer layers. Besides this, the XRD and UV–VIS spectra of the modified polymer layers and Tb_{NPS} were studied. In addition, the ESI method for bare and Tb_{NPs}@ poly m-THB/PGE was examined.

2.7. Validation Data

The proposed SWV method was validated following the ICH guidelines [38] for linearity range, the limit of detection (LOD), the limit of quantification (LOQ), accuracy and precision. The LOD and LOQ values were determined using formulas 3 σ/S and 10 σ/S, respectively, where σ represents the standard deviation of the intercept and S is the slope of the related regression equation. The electrochemical technique's precision was examined using three different concentrations within the calibration range within the same day (intra-day precision) and across three successive days (inter-day precision). The mean values of relative standard deviations (RSD%) of the results were calculated.

3. Results

3.1. Preparation of Tb_{NPS}@ Poly m-THB/PGE

The present research is the first to investigate the electrochemical performance of phloroglucinol; an m-trihydroxy benzene compound (m-THB); on the peak current value of FAV; an antiviral regimen for COVID-19. Since modification of carbon-based electrodes is a promising step to improve electrode surface area and enhance its electron transfer, the electrochemical polymerization of m-THB was performed, which covers the surface of PGE. All experimental variables influencing the polymerization step were examined, such as m-THB concentration, potential, number of polymerization cycles and the scan rate. The concentration of m-THB has a great effect on the polymerization procedure and on the FAV current value. So, concentrations of m-THB from 0.002 to 0.012 M were studied, where the current value was increased by increasing the concentration till constant values of current were obtained using concentrations from 0.007 to 0.009 M, after that, a decrease in current value was found as the resultant polymer film using higher concentration may block the surface of the formed electrode and hence decrease current intensity (Figure 1A). Hence, 0.008 M was selected as the optimum concentration of m-THB and was subsequently used for further measurements. After that, the potential range necessary for m-THB polymerization was tested using different potential values ranging from −0.2 to −1.6 V. An

increase in the current value of FAV was obtained by decreasing the potential value until a fixed current value was found at −0.8 V, and it was selected for further electrochemical measurements as represented in Figure 1B.

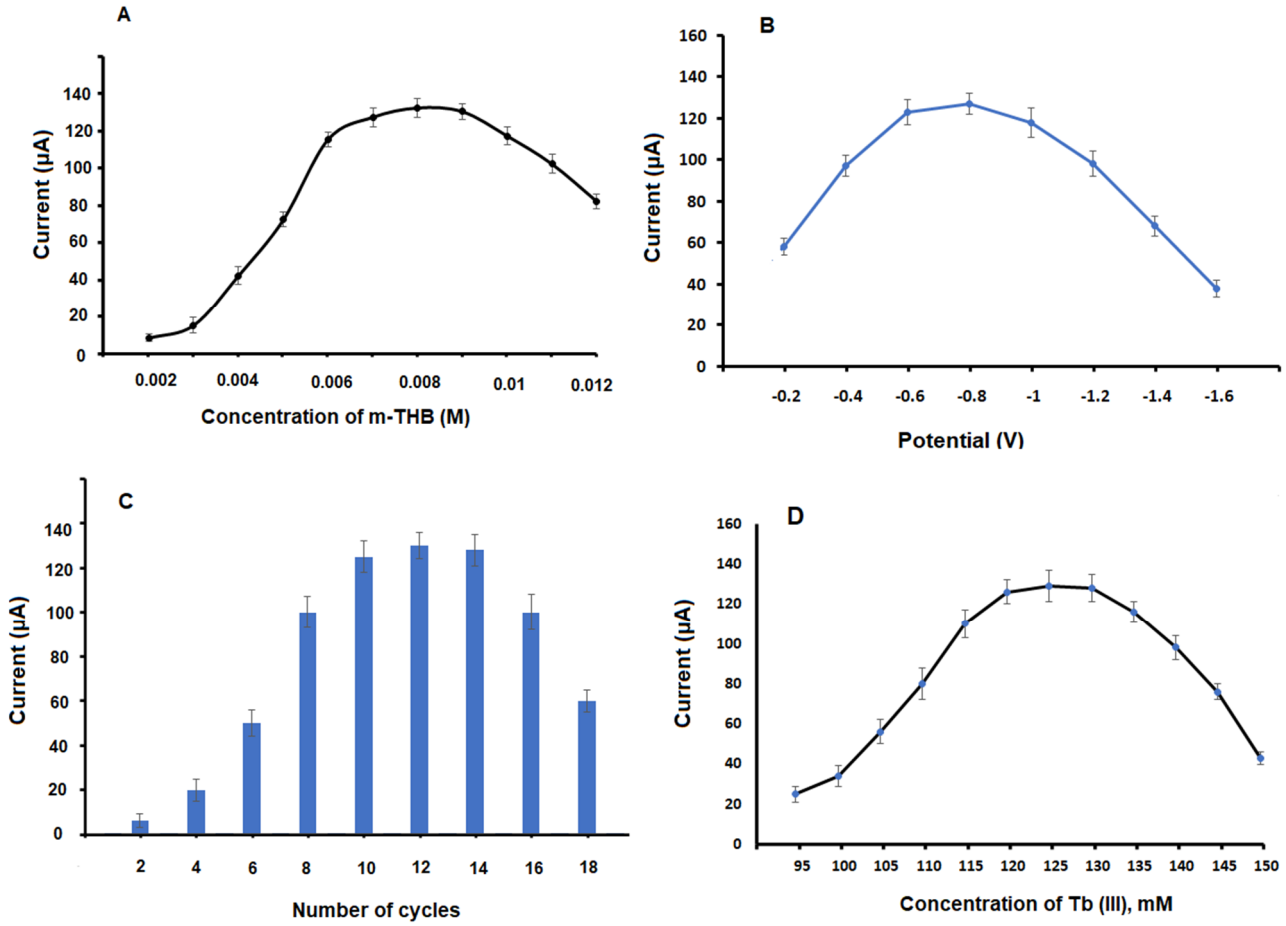


Figure 1. The effects of: (**A**) concentration of m-THB, (**B**) potential used in the polymerization of m-THB, (**C**) number of cycles for polymerization of m-THB and (**D**) concentration of Tb (III) on the current value of FAV (70×10^{-9} M) using Tb_{NPS} @ poly m-THB/PGE.

Owing to the importance of the number of cycles in the polymerization step, as it significantly affects electrode electro-catalytic activity, various numbers of cycles were performed. From data represented in Figure 1C, it was found that 12 cycles showed the highest values and a further decrease in current value was obtained using the number of cycles higher than 12. The scan rate was further tested from 0.05 to 0.4 V s^{-1}, and the highest peak current value was observed at 0.1 V $s^{-1,}$ as represented in Figure S1A (Supplementary Materials).

The formed polymer layers, poly m-THB over the PGE surface, were used as a platform for further loading of Tb_{NPS}, where an electro-deposition of Tb (III) solution was performed. Different concentrations of Tb (III) ranging from 95 to 150 mM were examined; it was observed that the highest and most stable results were obtained using 125 mM, as shown in Figure 1D. Further, deposition potential values required from −1.8 to −0.4 V and various deposition time from 10 to 120 s was examined. It was noticed that −1.2 V and 80 s showed the highest values, and they were used as the optimum parameters, as shown in Figure S1B (Supplementary Materials).

3.2. Electrochemical Performance of FAV at Bare and Modified PGE

The electro-oxidation of FAV was established at bare and modified PGE by both CV and SWV techniques. Figure 2A shows the distinct oxidation peak of FAV (70×10^{-9} M) at potential 1.14 V using bare PGE (curve a), poly m-THB/PGE (curve b) in 0.1 M phosphate buffer,

pH 7.0. The oxidation current values of FAV were 45 and 75 µA, respectively. Furthermore, Figure 2A (curve c) represented the deposition of Tb nanocomposites over poly m-THB/PGE surface, which remarkably enhanced the sensitivity towards FAV electro-oxidation, giving a higher current value (~127 µA) in comparison with bare PGE or poly m-THB/PGE which may be attributed to their good electro-activity, large surface areas and rapid transfer rate on the modified electrode surface. These findings clearly confirm the synergistic effect of the used hybrid composites, m-THB polymer and Tb $_{NPS}$, in electrode composition.

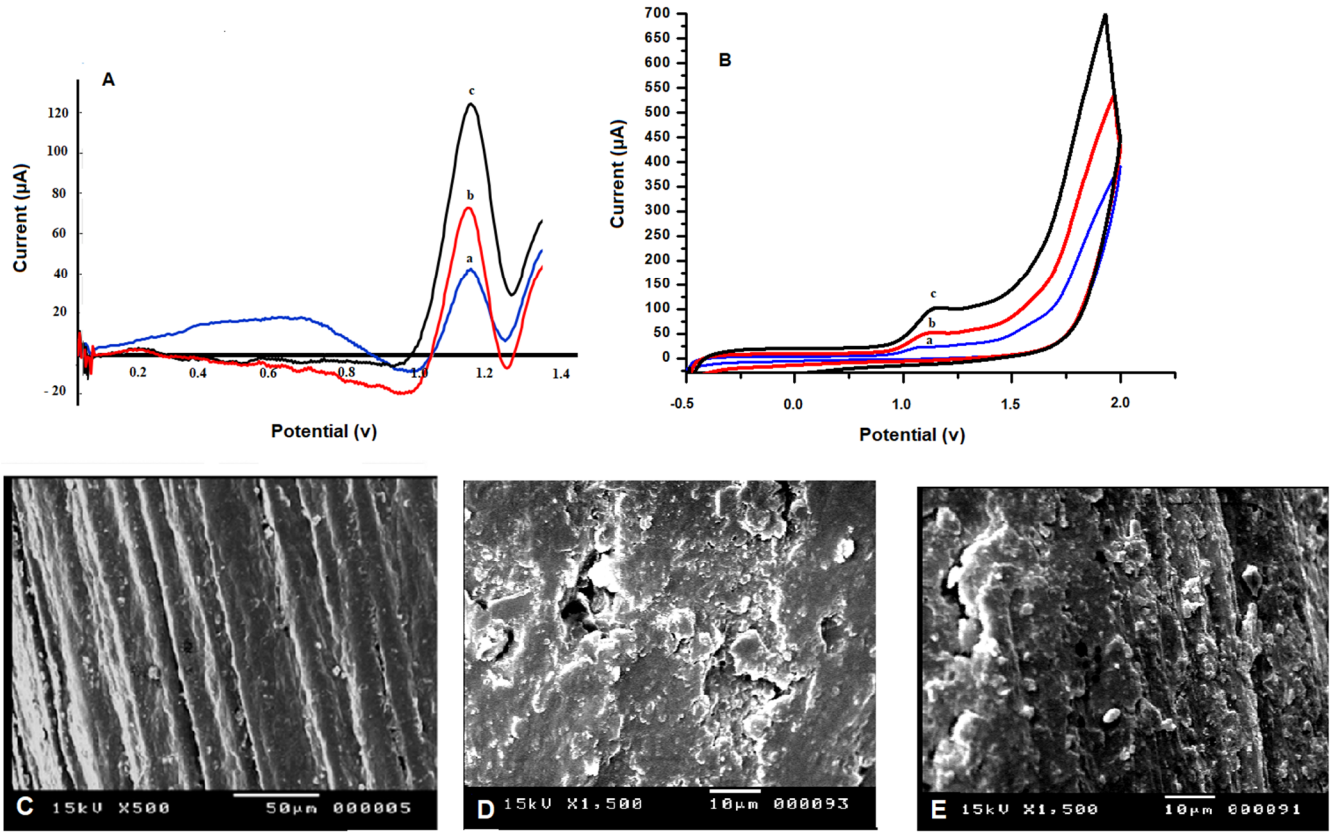


Figure 2. (**A**) SWVs, (**B**) CVs curves of FAV (70 × 10^{-9} M) recorded on: (a) bare PGE, (b) poly m-THB/PGE and (c) Tb_{NPS}@ poly m-THB/PGE & SEM images of: (**C**) bare PEG, (**D**) poly m-THB/PGE, and (**E**) Tb $_{NPS}$@ poly m-THB/PGE surface.

3.3. Characterization of Tb_{NPs}@ Poly m-THB/PGE

The morphological characterization of the fabricated electrodes was carried out by SEM technique, where SEM images of poly m-THB and Tb_{NPs}@ poly m-THB were represented in Figure 2. The SEM images of the bare PGE electrode are represented in Figure 2C, where distinguishable smooth layers [32] covering its surface can be observed. However, after polymerization with m-THB, obvious lumps and flake-like structures were observed coating the surface of the modified electrode, as shown in Figure 2D. After incorporation of Tb_{NPS} over the surface of poly m-THB/PGE electrode, characteristic lumps and depressions structures with glowing clusters were observed over the surface of the modified electrode Tb_{NPS} @ poly m-THB/PGE electrode as shown in Figure 2E.

The used modification forms porous structures covering the electrode surface, which improves the active surface area of the electrode and enhances FAV oxidation. Moreover, the XRD pattern showed diffraction peaks centered around values of 28.76_and 47.50, which are in agreement with the diagnostic peaks of Tb, as shown in Figure S2A.

Figure S2B (Supplementary Materials) represents the UV spectra of m-THB, Tb and Tb_{NPs}@ poly m-THB hybrid composite. As shown by curve i, a distinguished maximum peak of m-THB was observed at 268 nm. In addition, a characteristic peak of Tb was found

at ~220 nm, as represented in curve ii. In curve iii (spectrum of Tb_{NPs}@ poly m-THB hybrid modifier), another peak appeared at ~330 nm, which confirms the success of polymerization of m-THB, besides the characteristic peak of Tb at ~220 nm.

3.4. Investigation of Scan Rate

The investigation of the scan rate on the oxidation peak current of FAV in phosphate buffer (0.1 M, pH 7.0) using the fabricated electrode was performed by examining the related CV voltammograms at various scan rates from 100 to 900 mV/s. The peak current values of FAV were directly proportional to the scan rate, as shown in Figure 3, conforming Randles-Ševćik equation [39]. Figure 3A represents the enhancement in the anodic peak current by increasing the scan rate from 100 to 900 mV/s. The relationship between the oxidation peak current (*Ip*) and the scan rate (υ) showed a linear response following the equation below:

$$Ip\ (\mu A) = 15.8 + 121.7\ \upsilon \qquad (r^2 = 0.9924)$$

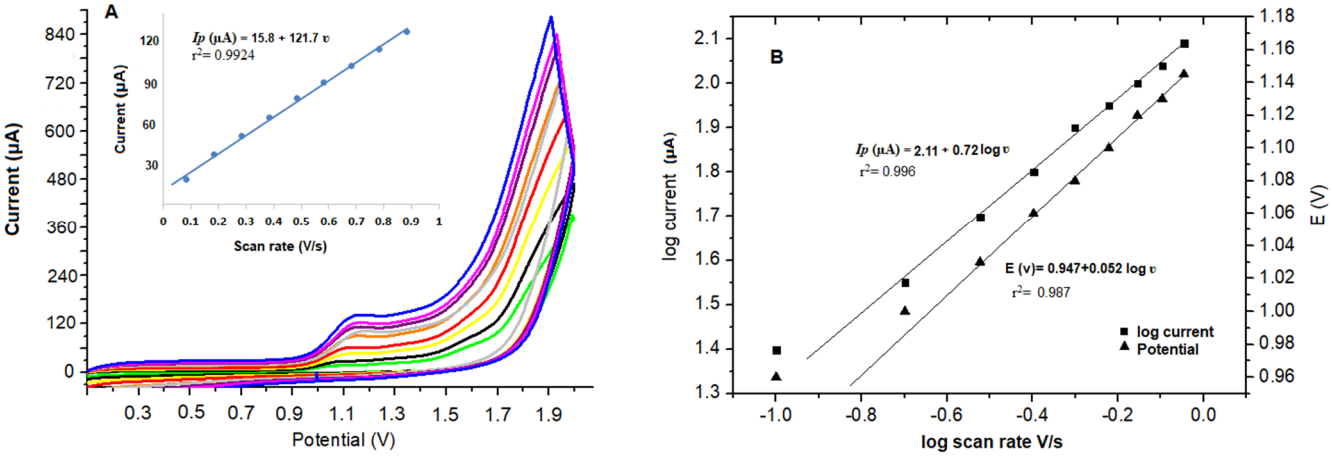


Figure 3. (**A**) The effect of different scan rates from 0.1 to 0.9 V s^{-1} on CVs curves of FAV (70×10^{-9} mol L^{-1}), Inset: Scan rate calibration plot and (**B**) Dependence of logarithm peak current ($Ip/\mu A$) and the oxidation peak potential (E/V) on the logarithm of scan rate (log ν/Vs^{-1}).

From Figure 3A, by increasing the scan rate, the oxidation potential of FAV was moved to more positive values, with an increase in the current intensity ensuring the irreversibility of the oxidation process of FAV. From data represented in Figure 3B, a plot of the logarithm of the oxidation peak current (log *Ip*) versus the logarithm of the scan rate (log υ) was found to be linear and was described by the following regression equation:

$$\log Ip\ (\mu A) = 2.11 + 0.72 \log \upsilon\ (V\ s^{-1}) \qquad (r^2 = 0.996)$$

The slope of the linear equation between log *Ip* versus log υ was 0.72. Hence the oxidation process of FAV is controlled by both adsorption and diffusion mechanisms, which agrees with the previous studies [18–21].

Further, by plotting potential (*Ep*) against the logarithm of scan rate (log υ), a linear relationship was obtained as represented in Figure 3B and described with the following regression equation:

$$E_p\ (V) = 0.947 + 0.052 \log \upsilon\ (V\ s^{-1}) \qquad (r^2 = 0.987)$$

As represented in Figure 2B, no cathodic peak for FAV was observed in the CV reverse scan, confirming the irreversibility of the oxidation reaction of FAV. Based on the Laviron

equation [40], the potential (E), number of transferred electrons (n) and scan rate in the rate-limiting step can be calculated from:

$$\text{The slope of the plot } E_p \text{ (V) and log } \upsilon = 2.2303\ RT/\alpha n\ F$$

T is the absolute temperature (298 K), n is the number of transferred electrons in the rate-determining step, R is the universal gas constant (8.314 J mol^{-1} K^{-1}) and F is the Faraday constant (96.480 C mol^{-1}). Assuming α (the transfer coefficient) is 0.5 in totally irreversible reactions, and after substitution of the slope with 0.052, the number of electrons involved in the oxidation process was calculated to be ≈2.0; this agrees with previously reported articles [20,21]. The oxidation reaction of FAV probably occurs in the aromatic hydroxyl group on the pyrazine ring in the FAV chemical structure, as mentioned before [19,20].

3.5. Electrochemical Characterization of Tb_{NPs}@ Poly m-THB/PGE

The electrochemical activity of Tb_{NPs}@ poly m-THB/PGE was examined using the CV technique, where Fe^{2+}/Fe^{3+} solution (1.0 mmol L^{-1}) prepared in 0.5 M of potassium chloride was used. After using the modified sensor, an increment in peak current intensity in the reduction-oxidation peak of the Fe^{2+}/Fe^{3+} system was observed, as represented in Figure 4A. This increment is due to an increase in the active surface area of the electrode after modification. This finding was affirmed by the EIS study, where measurements were performed at 10 mV, and the potential amplitude was within the frequency range (1.0–10 KHz). Tb_{NPs}@ poly m-THB/PGE electrode showed lower series resistance than that of the bare one. Moreover, the results in Figure 4B shows that bare PGE has displayed a semi-circular model, but Tb_{NPs}@ poly m-THB/PGE modified electrode displayed a straight linear curve. This indicates the improvement in the electrical conductivity due to the charge transfer acceleration and the surface area enlargement. In order to confirm this hypothesis, the electrode's active surface area was calculated using the Randles–Ševćik equation from the slope of anodic peak current (I_p):

$$I_{pa} = (2.69 \times 10^5)\ n^{3/2} A_{eff} D_R{}^{1/2} C_0 \upsilon^{1/2}$$

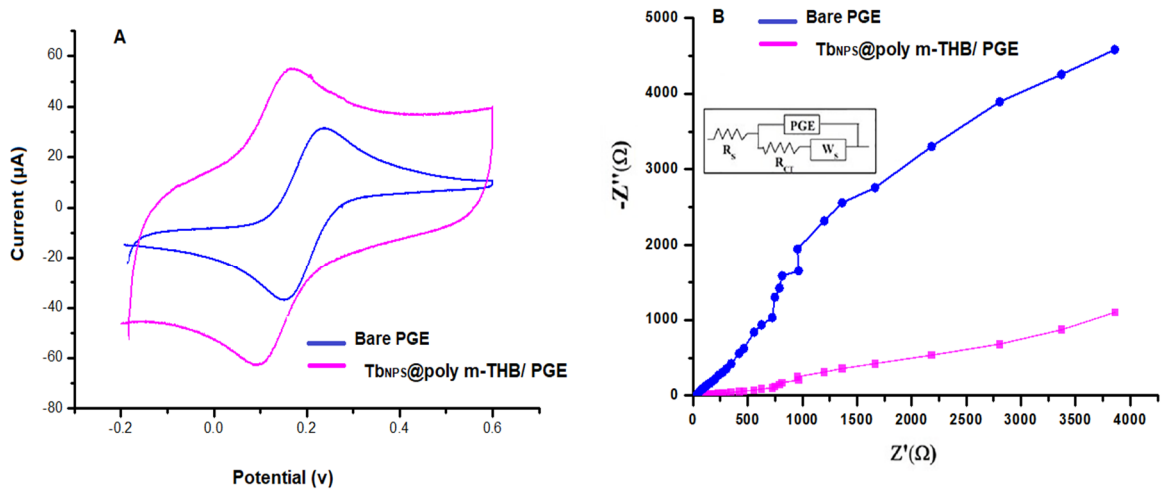


Figure 4. (**A**) Cyclic voltammograms and (**B**) Nyquist plot of 1.0 mM of Fe^{3+}/Fe^{2+} solution recorded on bare PGE and Tb_{NPS}@ poly m-THB/PGE electrodes. Working parameters are: scan rate 50 mV s^{-1} over a potential range of −0.2–0.6 V.

A_{eff} is the electrode surface area in cm^2, n is the number of electron transfers, D_R is the diffusion coefficient (cm^2 s^{-1}), C_0 is the concentration of Fe^{2+}/Fe^{3+} system (mol/cm^2) and υ is the scan rate (V s^{-1}). According to the Randles–Ševćik equation, the active surface areas of bare PGE and Tb_{NPs}@ poly m-THB/PGE have been calculated to be: 0.212 and

0.454 cm^2. This finding confirmed the improvement action of using the hybrid modification (m-THB polymer layers and Tb_{NPS}) regarding the oxidation of FAV using a Tb_{NPs}@ poly m-THB/PGE electrode.

3.6. Optimization of Method's Parameters

3.6.1. Effect of pH

Supporting electrolyte pH is very important to study the electrochemical behavior of FAV at the modified electrode. Therefore, different phosphate buffer solutions (0.1 M) from pH 4.0 to 9.0 were examined. An increase in the current value is observed by increasing the pH value. A phosphate buffer of pH 7.0 showed the highest value, and it was selected for further measurements, as represented in Figure S3A (Supplementary Materials). FAV molecule has two tautomeric forms, a more stable enol form and a ketone form, and the intersection point of the Ep/pH curves with a clear change in the peak intensity at about 7.0–8.0 may be explained by the replacement of one mechanism (reaction with enol) by another (reaction with ketone) in the tautomeric equilibrium of FAV. A linear plot between the pH values and their corresponding potential was represented in Figure S3B (Supplementary Materials), where the potential of the FAV oxidation peak was moved to less positive potential values upon increasing the pH value. It is noteworthy that Ep (V) = 1.122 + 0.053 pH (r = 0.994), which reveals the proton-dependent nature of FAV on the modified electrode. The value of the slope is close to the theoretical value of 59 mV; hence the number of electrons and protons involved in the electrochemical oxidation of FAV are equal. These findings are in agreement with the number of electrons (≈ 2.0 electrons) included in the oxidation of FAV, which is calculated above using the Laviron equation, and also in agreement with previously reported methods [19–22].

3.6.2. SWV Parameters

Instrumental parameters affecting the proposed SWV, such as pulse height, step height and frequency, were studied in the ranges 3–30 mV, 1–30 mV and 25–250 V s^{-1}, respectively. It was observed that pulse height at 5 mV, step height at 3 mV and frequency at 100 V s^{-1} were the optimal variables for electro-oxidation of FAV at the modified electrode. Besides, the initial potential and deposition time parameters of FAV were examined from −1.2 to + 0.8 V and from 10 to 90 s, and optimum values were −0.2 V and 60 s, respectively.

3.7. Validation Study

3.7.1. Linearity and Sensitivity Limits

The calibration curve of FAV over a concentration range from 10–150 × 10^{-9} M was constructed under the optimum conditions as represented in Figure S4 (Supplementary Materials). The values of LOD and LOQ were 3.1 and 9.3 × 10^{-9} M, respectively. Various statistical parameters of the proposed SWV method are represented in Table 1. The proposed method showed higher sensitivity than various previously reported methods.

Table 1. Linearity results for FAV determination by the proposed SWV method using Tb_{NPS}@ poly m-THB/PGE electrode.

Parameter	FAV
Linearity range (×10^{-9} M)	10–150
Correlation coefficient (r)	0.9994
Intercept (a) ± SD *	1.46 ± 2.33
Slope (b) ± SD *	2.5 ± 0.04
LOD ** (×10^{-9} M)	3.08
LOQ ** (×10^{-9} M)	9.32

* Average of four replicates. ** Detection (LOD) and quantification (LOQ) limits were calculated as 3.3 σ/b and 10 σ/b, respectively, where σ is the standard deviation of the intercept of the regression equation and b is the slope of the calibration curve.

3.7.2. Accuracy and Precision

The accuracy, repeatability and intermediate inter-day precisions for the proposed method were investigated. Table 2 summarizes the obtained results. The intra-day precision was evaluated by repeating the measurements of three various concentration levels of FAV working solutions (20, 70 and 120 $\times$ 10^{-9} M). The measurements were repeated over three consecutive days to examine the inter-day precision. Recovery results were observed to be from 98.92 to 101.42%, indicating acceptable accuracy. In addition, the % RSD values were calculated, and the results were less than 1.8%.

Table 2. Accuracy and precision results for determination of FAV under the developed SWV method.

Authentic Drug	Conc. ($\times 10^{-9}$ M)	Accuracy		Intra-Day Precision		Inter-Day Precision	
		% Recovery *	%RSD *	% Recovery *	%RSD *	%Recovery *	% RSD *
FAV	20	100.36	1.25	99.53	0.99	100.64	1.77
	70	98.92	0.93	101.42	1.81	101.32	1.34
	120	101.14	1.36	100.16	1.43	99.75	1.11

* Average of three replicates; Results are compared with those of the standard calibration curve.

3.7.3. Selectivity

The effect of commonly co-existing interfering substances during FAV analysis was examined in order to evaluate the selectivity of the fabricated Tb_{NPS}@ poly m-THB/PGE electrode. The concentration of each substance was tested at 10 folds the concentration of the drug used during the electrochemical measurement. The percentage recovery values were in the range of 96.8–100.2% in the presence of various substances ensuring high selectivity of the proposed SWV method for FAV estimation (Table 3).

Table 3. Selectivity of the proposed SWV method for determination of FAV.

Interfering Material	Inter-Day Precision	
	% Recovery *	% RSD *
Uric acid	99.3	1.2
Oxalic acid	100.2	0.9
Sucrose	97.3	1.1
Starch	99.1	1.4
Magnesium chloride	97.7	1.3
Citric acid	96.8	1.5
L-Ascorbic acid	97.2	1.7

* Average of three replicates; FAV: Interfering substance (1: 10).

3.8. Method Applications

3.8.1. Estimation of FAV in Pharmaceutical Tablet

The fabricated Tb_{NPS}@ poly m-THB/PGE electrode showed high sensitivity (LOD = 3.1 $\times$ 10^{-9} M); hence it was successfully used to determine FAV in commercial tablets. Acceptable recovery results were obtained, ranging from 99.58–100.93% $\pm$ 1.2–1.9, ensuring the absence of interference from commonly used excipients, as represented in Table 4. The obtained percentage recovery results were statistically compared to those calculated according to a previously published method [7]. The % recovery of the proposed method was 98.9 $\pm$ 1.2 when compared with that of the reported one (97.5 $\pm$ 1.6). Moreover, the calculated values of the *t*- and *F*-tests (n = 5) were 0.63 and 2.35, respectively, ensuring a lack of significant difference between the proposed and the published methods.

Table 4. Determination of FAV in tablets and human plasma using Tb_{NPS}@ poly m-THB/PGE electrode.

Sample	Added Amount (nM)	Found Concentration (nM)	%Recovery [a] ± %RSD	
Avipiravir® Tablet	20	20.09	100.45 ± 1.2	
	80	78.87	98.58 ± 1.6	
	120	121.12	100.93 ± 1.9	
Human plasma	30	29.56	98.53 ± 2.1	
	50	50.07	100.14 ± 1.8	
	70	71.35	101.93 ± 1.5	
	120	116.87	97.39 ± 1.7	
Proposed method		Reported method [8]	t-value [b]	F-Value [b]
98.9 ± 1.2		97.5 ± 1.6	0.63	2.35

[a] Average of three replicates. [b] Theoretical values at 95% confidence limit; t = 2.228, F = 5.053; (n = 6).

3.8.2. Estimation of FAV in Human Plasma

The fabricated electrode Tb_{NPS}@ poly m-THB/PGE was employed for FAV quantitation in human plasma, where a calibration curve of human plasma samples spiked with FAV was constructed in concentrations ranging from 15 to 90 × 10^{-9} M to assess linearity. A good linearity was obtained with a correlation coefficient equal to 0.9994. The regression equation is Y = 0.81 + 2.04 X (n = 3); Y is the current value, and X is FAV concentration.

Moreover, % recovery was calculated, and the results ranged from 97.39 to 101.93% with RSD% values less than 2.5, as represented in Table 4. The acceptable results confirm the efficiency of the established SWV method utilizing Tb_{NPS}@ poly m-THB/PGE for the detection of FAV without interferences from plasma constituents. The results obtained confirm the method's sensitivity and applicability for the determination of FAV in human plasma samples.

3.9. Stability and Reproducibility of the Fabricated Sensor

The stability of the modified Tb_{NPS}@ poly m-THB/PGE electro-sensor was examined, where the sensor was stored at 4 °C for 20 successive days, and the electrochemical behavior of FAV was assessed every 2 days. The storage stability of Tb_{NPS}@ poly m-THB/PGE was illustrated by the measured current (Figure S5A, Supplementary Materials) with a 98.53% retention of the original, optimized current values. Moreover, FAV (70 × 10^{-9} M) was analyzed using six parallel-prepared modified electrodes fabricated using the same procedure. The corresponding RSD% value didn't exceed 2.1% during the analysis, which proves the good reproducibility of the modified sensor, as shown in Figure S5B, Supplementary Materials.

The presented SWV method showed simplicity, good selectivity and high sensitivity utilizing the novel electrode (Tb_{NPS}@ poly m-THB/PGE) in comparison with previously published articles, as represented in Table 5. Some of the reported methods suffered from several demerits like insufficient sensitivity, complicated procedures or the need for large amounts of organic solvents. This confirms the excellent applicability of the proposed SWV for drug analysis in different media.

Table 5. Comparison between the proposed method for determination of FAV to previously reported methods.

Technique	Linearity Range	LOD	Application	Ref.
HPLC	0.5–50 µg/mL	0.04 µg/mL	Tablet	[5]
Spectrofluorimetry	40–280 ng/mL	9.44 ng/mL	Tablet/human plasma	[6]
Synchronous Fluorimetry	1–18 ng/mL	0.25 ng/mL	Tablet/human plasma	[8]
HPTLC	3.75–100 µg/mL	1.12 µg/mL	Pure form/Tablet	[11]
HPLC-UV	10–100 µg/mL	1.2 µg/mL	Tablet	[12]
HPLC-DAD	6.25–250 µg/mL	1.02 µg/mL	Tablet	[13]
UPLC-MS/MS	0.25–16 µg/mL	0.075 µg/mL	Human plasma	[14]
LC-MS/MS	0.048–50 µg/mL	0.045 µg/mL	Human serum	[17]
LC-MS/MS	0.1–20 µg/mL	0.03 µg/mL	Tablet &plasma	[15]
UPLC	0.1–10 µg/mL	0.03 µg/mL	Human plasma	[16]
SWV	0.01–0.1 µg/mL 0.1–20 µg/mL	3 ng/mL	Tablet/human urine	[18]
SWV	1.56–31.2 µg/mL	0.76 ng/mL	Tablet/serum	[19]
SWV	864–0.157 µg/mL	0.017 µg/mL	Tablet/urine	[22]
DPV	0.014–0.31 µg/mL	0.072 ng/mL	Tablet/plasma & urine	[20]
SWV	1–100 µg/mL	0.26 µg/mL	Tablet/urine	[21]
SWV	1.57–23.6 ng/mL	0.486 ng/mL	Tablets & human plasma	Proposed study

4. Conclusions

An innovative and highly sensitive electrochemical sensor was fabricated based on utilizing Tb nanoparticles supported over new polymer layers of m-THB. The performance of the fabricated sensor was examined for studying the electro-oxidation of FAV using the SWV technique. CV, SEM, XRD, UV-spectrophotometry and EIS techniques were conducted for further characterization. Tb_{NPs} and poly m-THB had synergistic effects, which enhanced the determination of FAV in tablets and in human plasma. A full validation study of the proposed method was carried out according to the ICH guidelines. The proposed sensor showed good recovery results for the demonstration of FAV in different matrices without any interference. Besides, it has high sensitivity and simplicity in fabrication, and this ensured good performance of fabricated senor in FAV determination in complex matrices. Notably, this study is the first to be reported for the investigation of the electrochemical performance of the modified electrode (Tb_{NPS} @poly m-THB/PGE) in the analysis of FAV.

Supplementary Materials: The following supporting information can be downloaded at: https://www.mdpi.com/article/10.3390/bios13020243/s1, Figure S1: Effect of (A) scan rate on the current of FAV (70×10^{-9} M) in electro-polymerization process of m-THB, and (B) deposition potential of Tb (III) solution; Figure S2: (A) XRD spectrum of Tb nanoparticles and (B) Uv spectra of: (i) m-THB, (ii) Tb and (iii) poly m-THB& Tb hybrid composite; Figure S3: (A) The effect of pH of supporting electrolyte pH on the oxidation peak of FAV (70×10^{-9} M), and (B) Linear plot between potential and pH values of the supporting electrolytes; Figure S4: Square wave voltammograms for various concentrations of FAV ($10–150 \times 10^{-9}$ M) monitored on Tb_{NPS}@ poly m-THB/PGE electrode.; Figure S5: Bar diagram curves obtained for (A) stability studies of Tb_{NPS}@ poly m-THB/PGE modified electrode over 20 days and (B) recording six different times to attain reproducibility study of Tb_{NPS}@ poly m-THB/PGE in the presence of FAV (70×10^{-9} M).

Author Contributions: Conceptualization, M.F.B.A. and A.E.I.; methodology, M.F.B.A. and B.I.S.; software, M.F.B.A. and A.E.I.; validation, M.F.B.A., R.E.S. and B.I.S.; formal analysis, R.E.S. and B.I.S.; investigation, R.E.S. and A.E.I.; resources, R.E.S., B.I.S. and A.E.I.; data curation, R.E.S. and A.E.I.; writing—original draft preparation, R.E.S., B.I.S. and M.F.B.A.; writing—review and editing, B.I.S., M.F.B.A. and A.E.I.; visualization, M.F.B.A. and S.E.D.; supervision, M.F.B.A. and S.E.D.; project administration, M.F.B.A. and S.E.D.; funding acquisition, S.E.D. All authors have read and agreed to the published version of the manuscript.

Funding: This research received no external funding.

Institutional Review Board Statement: Not applicable.

Informed Consent Statement: Not applicable.

Data Availability Statement: All data are available from the corresponding author upon reasonable request.

Conflicts of Interest: The authors declare no conflict of interest.

References

1. Joshi, S.; Parkar, J.; Ansari, A.; Vora, A.; Talwar, D.; Tiwaskar, M.; Patil, S.; Barkate, H. Role of favipiravir in the treatment of COVID-19. *Int. J. Infect. Dis.* **2021**, *102*, 501–508. [CrossRef]
2. Cai, Q.; Yang, M.; Liu, D.; Chen, J.; Shu, D.; Xia, J.; Liao, X.; Gu, Y.; Cai, Q.; Yang, Y. Experimental treatment with favipiravir for COVID-19: An open-label control study. *Engineering* **2020**, *6*, 1192–1198. [CrossRef]
3. Ioannidis, J.P.A. The end of the COVID-19 pandemic. *Eur. J. Clin. Investig.* **2022**, *52*, e13782. [CrossRef]
4. Murray, C.J. COVID-19 will continue but the end of the pandemic is near. *Lancet* **2022**, *399*, 417–419. [CrossRef]
5. Sharaf, Y.A.; El Deeb, S.; Ibrahim, A.E.; Al-Harrasi, A.; Sayed, R.A. Two Green Micellar HPLC and Mathematically Assisted UV Spectroscopic Methods for the Simultaneous Determination of Molnupiravir and Favipiravir as a Novel Combined COVID-19 Antiviral Regimen. *Molecules* **2022**, *27*, 2330. [CrossRef]
6. Megahed, S.M.; Habib, A.A.; Hammad, S.F.; Kamal, A.H. Experimental design approach for development of spectrofluorimetric method for determination of favipiravir; a potential therapeutic agent against COVID-19 virus: Application to spiked human plasma. *Spectrochim. Acta Part A Mol. Biomol. Spectrosc.* **2020**, *249*, 119241. [CrossRef]
7. Mikhail, I.E.; Elmansi, H.; Belal, F.; Ehab Ibrahim, A. Green micellar solvent-free HPLC and spectrofluorimetric determination of favipiravir as one of COVID-19 antiviral regimens. *Microchem. J.* **2021**, *165*, 106189. [CrossRef]
8. El Sharkasy, M.E.; Tolba, M.M.; Belal, F.; Walash, M.; Aboshabana, R. Quantitative analysis of favipiravir and hydroxychloroquine as FDA-approved drugs for treatment of COVID-19 using synchronous spectrofluorimetry: Application to pharmaceutical formulations and biological fluids. *Luminescence* **2022**, *37*, 953–964. [CrossRef]
9. Ibrahim, A.E.; Sharaf, Y.A.; El Deeb, S.; Sayed, R.A. Analytical Performance and Greenness Evaluation of Five Multi-Level Design Models Utilized for Impurity Profiling of Favipiravir, a Promising COVID-19 Antiviral Drug. *Molecules* **2022**, *27*, 3658. [CrossRef]
10. Noureldeen, D.A.M.; Boushra, J.M.; Lashien, A.S.; Hakiem, A.F.A.; Attia, T.Z. Novel environment friendly TLC-densitometric method for the determination of anti-coronavirus drugs "Remdesivir and Favipiravir": Green assessment with application to pharmaceutical formulations and human plasma. *Microchem. J.* **2022**, *174*, 107101. [CrossRef]
11. Saraya, R.E.; Deeb, S.E.; Salman, B.I.; Ibrahim, A.E. Highly sensitive high-performance thin-layer chromatography method for the simultaneous determination of molnupiravir, favipiravir, and ritonavir in pure forms and pharmaceutical formulations. *J. Sep. Sci.* **2022**, *45*, 2582–2590. [CrossRef]
12. Bulduk, İ. HPLC-UV method for quantification of favipiravir in pharmaceutical formulations. *Acta Chromatogr.* **2021**, *33*, 209–215. [CrossRef]
13. Marzouk, H.M.; Rezk, M.R.; Gouda, A.S.; Abdel-Megied, A.M. A Novel Stability-Indicating HPLC-DAD Method for Determination of Favipiravir, a Potential Antiviral Drug for COVID-19 Treatment; Application to Degradation Kinetic Studies and In-Vitro Dissolution Profiling. *Microchem. J.* **2022**, *172*, 106917. [CrossRef]
14. Rezk, M.R.; Badr, K.A.; Abdel-Naby, N.S.; Ayyad, M.M. A novel, rapid and simple UPLC–MS/MS method for quantification of favipiravir in human plasma: Application to a bioequivalence study. *Biomed. Chromatogr.* **2021**, *35*, e5098. [CrossRef]
15. Morsy, M.I.; Nouman, E.G.; Abdallah, Y.M.; Zainelabdeen, M.A.; Darwish, M.M.; Hassan, A.Y.; Gouda, A.S.; Rezk, M.R.; Abdel-Megied, A.M.; Marzouk, H.M. A novel LC-MS/MS method for determination of the potential antiviral candidate favipiravir for the emergency treatment of SARS-CoV-2 virus in human plasma: Application to a bioequivalence study in Egyptian human volunteers. *J. Pharm. Biomed. Anal.* **2021**, *199*, 114057. [CrossRef]
16. Emam, A.A.; Abdelaleem, E.A.; Abdelmomen, E.H.; Abdelmoety, R.H.; Abdelfatah, R.M. Rapid and ecofriendly UPLC quantification of Remdesivir, Favipiravir and Dexamethasone for accurate therapeutic drug monitoring in Covid-19 Patient's plasma. *Microchem. J.* **2022**, *179*, 107580. [CrossRef]
17. Onmaz, D.E.; Abusoglu, S.; Onmaz, M.; Yerlikaya, F.H.; Unlu, A. Development and validation of a sensitive, fast and simple LC-MS/MS method for the quantitation of favipiravir in human serum. *J. Chromatogr. B* **2021**, *1176*, 122768. [CrossRef]
18. Allahverdiyeva, S.; Yunusoğlu, O.; Yardım, Y.; Şentürk, Z. First electrochemical evaluation of favipiravir used as an antiviral option in the treatment of COVID-19: A study of its enhanced voltammetric determination in cationic surfactant media using a boron-doped diamond electrode. *Anal. Chim. Acta* **2021**, *1159*, 338418. [CrossRef]
19. Kanbeş Dindar, Ç.; Bozal-Palabiyik, B.; Uslu, B. Development of a Diamond Nanoparticles-based Nanosensor for Detection and Determination of Antiviral Drug Favipiravir. *Electroanalysis* **2022**, *34*, 1174–1186. [CrossRef]
20. Mehmandoust, M.; Khoshnavaz, Y.; Tuzen, M.; Erk, N. Voltammetric sensor based on bimetallic nanocomposite for determination of favipiravir as an antiviral drug. *Microchim. Acta* **2021**, *188*, 434. [CrossRef]
21. Akca, Z.; ÖZOK, H.İ.; Yardim, Y.; Şentürk, Z. Electroanalytical investigation and voltammetric quantification of antiviral drug favipiravir in the pharmaceutical formulation and urine sample using a glassy carbon electrode in anionic surfactant media. *Turk. J. Chem.* **2022**, *46*, 869–880. [CrossRef]

22. Mohamed, M.A.; Eldin, G.M.; Ismail, S.M.; Zine, N.; Elaissari, A.; Jaffrezic-Renault, N.; Errachid, A. Innovative electrochemical sensor for the precise determination of the new antiviral COVID-19 treatment Favipiravir in the presence of coadministered drugs. *J. Electroanal. Chem.* **2021**, *895*, 115422. [CrossRef]
23. El-Wekil, M.M.; Hayallah, A.M.; Abdelgawad, M.A.; Abourehab, M.A.; Shahin, R.Y. Nanocomposite of gold nanoparticles@ nickel disulfide-plant derived carbon for molecularly imprinted electrochemical determination of favipiravir. *J. Electroanal. Chem.* **2022**, *922*, 116745. [CrossRef]
24. Erçarıkcı, E.; Aksu, Z.; Topçu, E.; Kıranşan, K.D. ZnS Nanoparticles-decorated Composite Graphene Paper: A Novel Flexible Electrochemical Sensor for Detection of Dopamine. *Electroanalysis* **2022**, *34*, 91–102. [CrossRef]
25. Erçarıkcı, E.; Aksu, Z.; Dağcı Kıranşan, K.; Topçu, E. Graphene paper with electrodeposited NiCo2S4 nanoparticles as a novel flexible sensor for simultaneous detection of folic acid and ascorbic acid. *Diam. Relat. Mater.* **2022**, *121*, 108713. [CrossRef]
26. Abdel-aal, F.A.; Ali, M.F. Eco-friendly fabricated electrochemical sensor using red cabbage extract for electrochemical determination of dacarbazine with the aid of factorial design approach. *J. Electrochem. Soc.* **2017**, *164*, H1053. [CrossRef]
27. Ali, M.F.; El-Zahry, M.R. A comparative study of different electrodeposited NiCo 2 O 4 microspheres anchored on a reduced graphene oxide platform: Electrochemical sensor for anti-depressant drug venlafaxine. *RSC Adv.* **2019**, *9*, 31609–31620. [CrossRef]
28. El-Zahry, M.R.; Ali, M.F. A novel polymer integrated Vertically-Oriented reduced graphene oxide sheets supported over palladium nanoparticles based sensor for Real-Time monitoring of Sorafenib; a Multi-kinase inhibitor in complex biological samples. *Microchem. J.* **2022**, *180*, 107549. [CrossRef]
29. Zhao, X.; Chen, X.; Yu, X.; Ding, X.; Yu, X.; Tang, K. High sensitivity humidity sensor and its application in nondestructive testing for wet paper. *Sens. Actuators B Chem.* **2019**, *301*, 127048. [CrossRef]
30. Vishnu, N.; Gandhi, M.; Badhulika, S.; Kumar, A.S. Tea quality testing using 6B pencil lead as an electrochemical sensor. *Anal. Methods* **2018**, *10*, 2327–2336. [CrossRef]
31. Ramanaviciene, A.; Plikusiene, I. Polymers in Sensor and Biosensor Design. *Polymers* **2021**, *13*, 917. [CrossRef]
32. Hosny, N.M.; Ali, M.F. Emphasis on the incorporation of Tropaeolin OO dye and silver nanoparticles for voltammetric estimation of flibanserin in bulk form, tablets and human plasma. *Talanta* **2022**, *245*, 123420. [CrossRef]
33. Ali, M.F.; Abdel-Aal, F.A. In situ polymerization and FT-IR characterization of poly-glycine on pencil graphite electrode for sensitive determination of anti-emetic drug, granisetron in injections and human plasma. *RSC Adv.* **2019**, *9*, 4325–4335. [CrossRef]
34. Mahanthesha, K.; Swamy, B.K.; Chandra, U. Simultaneous determination of dopamine at poly (Pyrogallol) modified carbon paste electrode: A Voltammetric Study. *IJRAR-Int. J. Res. Anal. Rev. (IJRAR)* **2018**, *5*, 1252–1257.
35. Sukanya, R.; Sakthivel, M.; Chen, S.-M.; Chen, T.-W. A new type of terbium diselenide nano octagon integrated oxidized carbon nanofiber: An efficient electrode material for electrochemical detection of morin in the food sample. *Sens. Actuators B: Chem.* **2018**, *269*, 354–367. [CrossRef]
36. Baytak, A.K.; Duzmen, S.; Teker, T.; Aslanoglu, M. A novel modified electrode based on terbium oxide and carbon nanotubes for the simultaneous determination of methyldopa and paracetamol. *Anal. Methods* **2016**, *8*, 4711–4719. [CrossRef]
37. Gadallah, M.I.; Ali, H.R.H.; Askal, H.F.; Saleh, G.A. Development of terbium based sensor for determination of imipenem in dosage forms and real samples. *J. Mol. Liq.* **2019**, *276*, 705–713. [CrossRef]
38. ICH Harmonised Tripartite Guideline, Validation of Analytical Procedures: Text and Methodology, Q2 (R1) Geneva. 2005. Available online: http://www.ich.org (accessed on 6 June 2021).
39. Bard, A.J.; Faulkner, L.R.; White, H.S. *Electrochemical Methods: Fundamentals and Applications*; John Wiley & Sons: Hoboken, NJ, USA, 2022.
40. Laviron, E. General expression of the linear potential sweep voltammogram in the case of diffusionless electrochemical systems. *J. Electroanal. Chem. Interfacial Electrochem.* **1979**, *101*, 19–28. [CrossRef]

Disclaimer/Publisher's Note: The statements, opinions and data contained in all publications are solely those of the individual author(s) and contributor(s) and not of MDPI and/or the editor(s). MDPI and/or the editor(s) disclaim responsibility for any injury to people or property resulting from any ideas, methods, instructions or products referred to in the content.